CORRELATION ESTIMATOR FOR TWO-CHANNEL, NON-COINCIDENCE LASER-DOPPLER-ANEMOMETER

H. Nobach[1], E. Müller[2], C. Tropea[3]

[1]Dantec Measurement Technology
Tonsbakken 16-18, 2740 Skovlunde, Denmark

[2]Universität Rostock, Fachbereich Elektrotechnik und Informationstechnik
Institut für Nachrichtentechnik und Informationselektronik
Richard-Wagner-Straße 31, 18119 Rostock, Germany

[3]FG Strömungslehre und Aerodynamik (SLA), Technische Universität Darmstadt
Petersenstr. 30, 64287 Darmstadt, Germany

ABSTRACT

Two new estimators are introduced for correlation functions between two or more channels of a laser Doppler anemometer (LDA). The first estimator is based on a slotting technique and the second on a sample-and-hold reconstruction with a refinement of the correlation estimate. In both cases the coincidence requirement between channels is eliminated. The estimators are applicable to two-component or three-component LDA, but is more interesting for two-point or multi-point LDA, where coincidence is practically non-existent or where the effective separation distance goes to zero for overlapping volumes, thus biasing the spatial correlation function at low separations.

1. INTRODUCTION

Two or multi-channel laser Doppler anemometry (LDA) is used when correlations between velocity fluctuations are required. In a two velocity component LDA, the two measurement volumes are at the same location in the flow and the correlations between components represent components of the Reynolds shear stress tensor. If a two-point or multi-point LDA is considered, the correlations then represent spatial correlations. Most commonly, these correlations between velocity fluctuations are evaluated at time lag zero (covariance or after normalization correlation coefficient), however in principle all time lags can be considered, in which case the correlation function or space-time correlation function between velocity fluctuations can be obtained.

There are three basic deficiencies in present LDA systems which can be eliminated using the new estimators for cross-correlations. The first concerns the need for coincidence. Conventional estimators of the cross-correlation function work directly from the definition

$$R_{AB}(\tau) = \frac{1}{N}\sum_{i=1}^{N} u_A(t_i)u_B(t_i+\tau) \qquad (1)$$

whereby it is understood that the mean has been removed from the input signals u_A and u_B. Thus a product $u_A u_B$ can only be contribute to the sum if velocity information from the two channels come with a time lag of exactly τ. Practically an acceptance window in time (coincidence window) is tolerated, however in many applications this window must be chosen very narrow to avoid a loss of correlation, hence a biased estimator. Physically, the required window width will be dictated by the time correlation function itself, and must often be chosen empirically and/or iteratively.

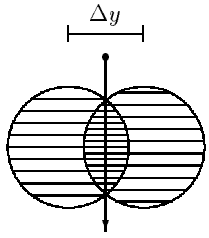

Figure 1: Two-point configuration leading to spatial bias of the cross-correlation funtion.

In any case, given a narrow coincidence window, the data rate of coincident velocity pairs may become very low, especially for spatially separated measurement volumes, which will be the focus of this paper. Thus, the duration of the measurement to achieve a statistically satisfactory number of samples N may become intolerably long. Accepting a lower value of N simply increases the variance of the estimate.

A second deficiency concerns the coincidence window implementation, which is available at the hardware level only for $\tau = 0$. In this case only data pairs which occur simultaneous in time are actively acquired, minimizing the amount of collected data. For other time lags ($\tau \neq 0$) no hardware coincidence is forseen. If the function $R_{AB}(\tau)$ is to be evaluated at many τ values, then all data must be acquired from both channels and coincidence must be implemented at the software level. In this case, again, due to the generally lower 'hit' rate of coincidence, large amounts of data must be acquired and recorded to yield statistically secure estimates.

A final difficulty with present estimators has been pointed out by Benedict and Gould [2] in their discussion of two-point correlation estimates when the separation distance becomes very small. Such measurements are necessary if direct measurements of dissipation are to be attempted. Once the two LDA measurement volumes begin to overlap any g-type correlation will become biased because coincidence will be triggered when a single particle passes through the overlapping region, as illustrated in figure 1. However velocity data from the two channels is not originating with the surmised spatial separation of Δy, but with an effective spatial separation of *zero*. Thus the estimator using coincidence will lead to a spatial bias in the near-field region. This bias is very significant, since the number of such single particle, two channel signals is much more frequent that two particle, two channel coincident signals.

All of the above difficulties will be alleviated using the new estimators. The next section describes briefly the simulation techniques used to produce test signals. The two new estimators for non-coincidence, cross-correlation are introduced in section 3. The performance of the estimators applied to two-point LDA is studied in section 4 and a discussion and conclusion are given in section 5.

2. SIGNAL SIMULATION

The results presented in this paper have been achieved using simulated signals, which allow systematic variation of influencing parameters and also evaluation of absolute errors, i.e. estimator biases. The techniques for generating a time-dependent, three-dimensional velocity field of given statistical characteristics have been introduced previously in [3]. Since in the present case a two-point LDA system is being examined, a spatial dependence must be added, with a given spatial correlation function. Details of how this was achieved can be found in [5].

The two situations which were examined are shown pictorially in figure 2 and correspond to a f-type and g-type correlation respectively. The main flow direction is along the x-axis and the mean velocity in both the y and z directions is zero. A cosine function was chosen to describe the spatial correlation with an integral length scale (first zero crossing) of 57 μm in the direction of the measurement volume separation and 1 m in the other two directions, the latter case making its influence negligible. The measurement volumes had dimensions of 40 μm (x) $\times$ 40 μm (y) $\times$ 40 μm (z). Although unrealistic at 40 μm , the length (z) has no particular consequence since there is no z velocity component and thus, together with the particle concentration, only the data rate is effected by this dimension.

An uncorrelated noise component could be added to the simulated velocity values. The simulation was then repeated for various values of measurement volume separation, either in x or y, for an f or g type correlation respectively. Two cases for each correlation type were investigated. The first case had a mean velocity of 10 m/s and a variance of 1 m^2/s^2, in which case 100 repititions of the simulations were used to enable the statistical certainty of the results to be established. The second case had a mean velocity of only 1 m/s, thus representing a much higher turbulence level.

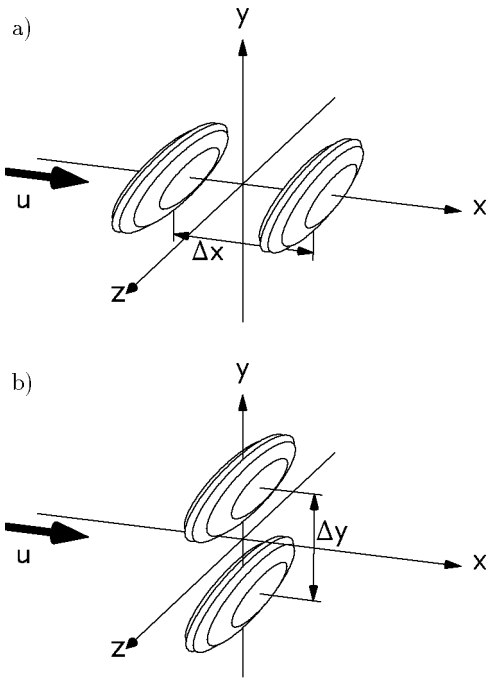

Figure 2: Measurement volume positions for signal simulation: a) f- type and b) g-type correlations.

The conditions of the four simulation cases are summerized in table 1.

3. DESCRIPTION OF ESTIMATORS

3.1 Coincidence based Estimator

For comparison purposes a software implementation of the conventional hardware coincidence was used to evaluate the coincidence based correlation given by

$$R_{AB}^{(c)}(0) = \frac{1}{N_c} \sum_{h=1}^{N_c} u_A(t_{Ah}) u_B(t_{Bh}) \tag{2}$$

where N_c is the number of coincidence events and the arrival times satisfy the relation

$$|t_{Ah} - t_{Bh}| < \tau_c. \tag{3}$$

The data rate of coincident events is denoted by $\dot{n}_c$.

3.2 Slot Correlation Estimator

The slot correlation estimator is given by

$$R_{AB}^{(s)}(k\Delta\tau) = \frac{\sum_{i=1}^{N_A} \sum_{j=1}^{N_B} u_{Ai} u_{Bj} b_k(t_{Bj} - t_{Ai})}{\sum_{i=1}^{N_A} \sum_{j=1}^{N_B} b_k(t_{Bj} - t_{Ai})} \tag{4}$$

where the weighting function b_k is given by

$$b_k(\Delta t) = \begin{cases} 1 - \left| \frac{\Delta t}{\Delta\tau} - k \right| & \text{for } \left| \frac{\Delta t}{\Delta\tau_c} - k \right| < 1 \\ 0 & \text{otherwise} \end{cases} \tag{5}$$

Correlation Case		f- type 1	f- type 2	g-type 3	g-type 4
Mean	m_u	10	1	10	1
velocity	m_v	0	0	0	0
[m/s]	m_w	0	0	0	0
Velocity	σ_u^2	1	1	1	1
variance	σ_v^2	0	0	0	0
[m^2/s^2]	σ_w^2	0	0	0	0
Reynolds	c_{uv}	0	0	0	0
stresses	c_{uw}	0	0	0	0
[m^2/s^2]	c_{vw}	0	0	0	0
Integral	I_u	40	400	40	400
time	I_v	–	–	–	–
scale [ms]	I_w	–	–	–	–
Integral	L_x	57.3 μm	57.3 μm	1 m	1 m
length	L_y	1 m	1 m	57.3 μm	57.3 μm
scale	L_z	1 m	1 m	1 m	1 m
Record length [s]	T	100	1000	100	1000
MV	$2a$	40	40	40	40
dimensions	$2b$	40	40	40	40
[μm]	$2c$	40	40	40	40
Coincidence time [μs]	τ_c	5	50	500	5000
Lag time interval [ms]	$\Delta\tau$	10	100	10	100
Particle conc. [m^{-3}]	c_p	3×10^9	3×10^9	3×10^9	3×10^9
Noise Level [m^2/s^2]	σ_N^2	0.1	0.001	0.1	0.001

Table 1: Summary of simulation parameters for data sets 1–4.

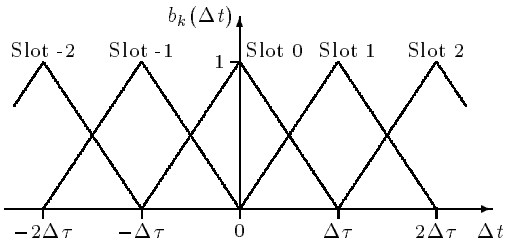

Figure 3: Illustration of weighting function $b_k(\Delta t)$.

and $\Delta t = t_{Bj} - t_{Ai}$. This weighting function is illustrated in figure 3 and represents a modification to conventional slot correlation estimates. Physically the slots are no longer sharply defined and this results in a lower variance of the correlation estimate, since slot quantisation noise is reduced.

The data rate, or *slot* rate, is denoted by $\dot{n}_s(k\Delta\tau)$.

3.3 Reconstruction based Estimator

Details of the estimator based on signal reconstruction can be found in [4]. A sample-and-hold (S+H) reconstruction has been employed with a re- sampling at the time intervals of $\Delta\tau$. The S+H can be represented by

$$\begin{aligned} u_A(t) &= u_{Ai} \qquad \forall \quad t_{Ai} \le t < t_{Ai+1} \\ u_B(t) &= u_{Bj} \qquad \forall \quad t_{Bj} \le t < t_{Bj+1} \end{aligned} \tag{6}$$

and the resulting cross-correlation estimator by

$$R_{AB}^{(n)}(k\Delta\tau) = \begin{cases} \frac{1}{N_r-k} \sum_{i=1}^{N_r-k} u_A(i\Delta\tau) u_B((i+k)\Delta\tau) \\ \qquad\qquad \text{for } k \ge 0 \\ \frac{1}{N_r-|k|} \sum_{i=1+|k|}^{N_r} u_A(i\Delta\tau) u_B((i-|k|)\Delta\tau) \\ \qquad\qquad \text{for } k < 0 \end{cases} \tag{7}$$

where N_r is the total number of resampled data points.

The low-pass filter associated with this reconstruction and re-sampling (eg. [1]) is compensated for by recognizing that the filter F can be inverted, i.e.

$$R_{AB}^{(r)} = F^{-1} R_{AB}^{(n)} \tag{8}$$

to yield an improved estimate of the cross-correlation function $R_{AB}^{(r)}$. This stage of the estimation has been termed refinement and has been initially formulated for autocorrelation function to improve frequency spectrum estimation from LDA data [6].

4. RESULTS

4.1 f-type Correlation

The results for case 1 (low velocity bias) are summarized in figure 4, showing the expectation and the data rates for the f-type correlation. In figure 4a the three estimates are compared to the theoretical spatial correlation (cosine). Also the reconstruction estimate without refinement has been added to this figure. The reconstruction technique exhibits a very low systematic error, with or without refinement. The refinement is not really necessary since almost all particles producing a signal in the first measurement volume also result in a signal in the second measurement volume (low turbulence).

The slot correlation lies consistently below the reconstruction estimate, due to multiple particle measurement in the slots. This can be seen by examining the data rates, as shown in figure 4b. The mean expected data rate at zero time lag is estimated from the particle concentration, the mean velocity and the projected measurement volume to be approximately 38 s^{-1}. Whereas the coincident estimator achieves about this value, the slot correlation lies significantly above. Thus cross-correlation contributions from different particles within a slot are being considered, which lowers the estimate marginally. Physically this means a small influence of the time correlation function is entering into the spatial correlation estimate.

The coincidence estimate performs very well up to a spatial separation corresponding to the overlapping of the measurement volumes. Due to the short coincidence time chosen (5 μs), the data falls off abruptly beyond this point. Only the fastest particles still fulfil the coincidence requirement, thus strongly biasing the correlation estimate.

The empirically determined variance of the reconstruction estimate was found to be the lowest (not shown).

Results for case 2 (high turbulence level) are shown in figure 5, in which all estimators are seen to be biased. This is an error associated with the classical velocity bias. As in the previous case, the coincident estimator undergoes a negative bias at larger separation, due to the selection of only fast particles through the coincidence window.

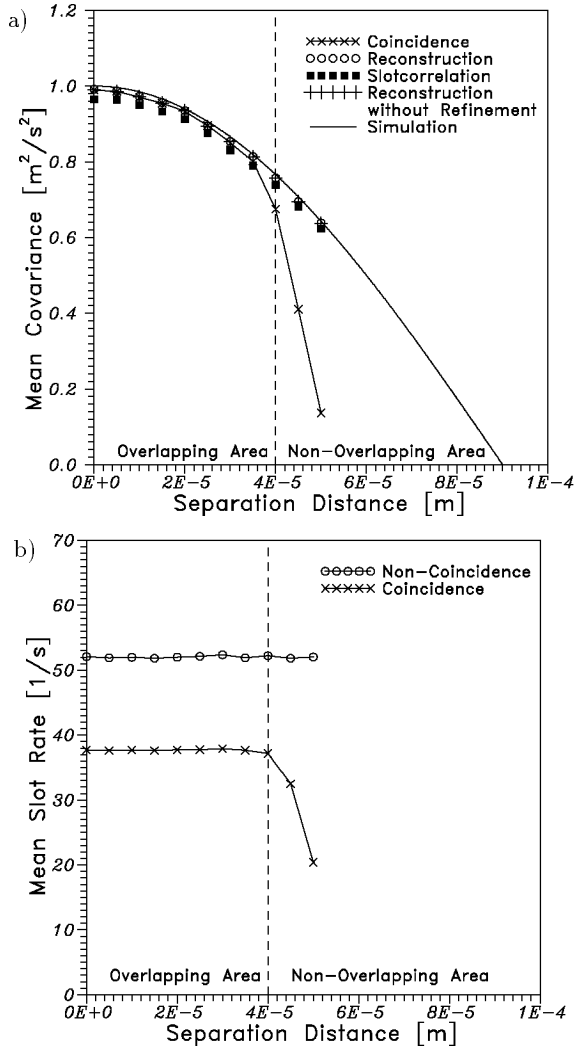

Figure 4: Results for case 1: low turbulence, f-type correlation.

The effect is not as abrupt in this case, only because the turbulence level is higher and the effect becomes 'smeared' out.

Again the variance of the reconstruction estimator is the lowest.

4.2 g-type Correlation

The results for the g-type correlation at low turbulence are summarized in the three diagrams of figure 6. In the diagram of the mean covariance (figure 6a), also the reconstruction estimate without refinement is shown and agrees well with results presented in [4].

The coincidence estimator exhibits a strong systematic error for spatial separations in which the measurement volumes still overlap. This corresponds to the problem outlined in conjunction with figure 1. Since the effective spatial separation remains effectively zero for overlapping volumes, the mean covariance maintains a value close to 1. For non-overlapping volumes, this estimate follows the

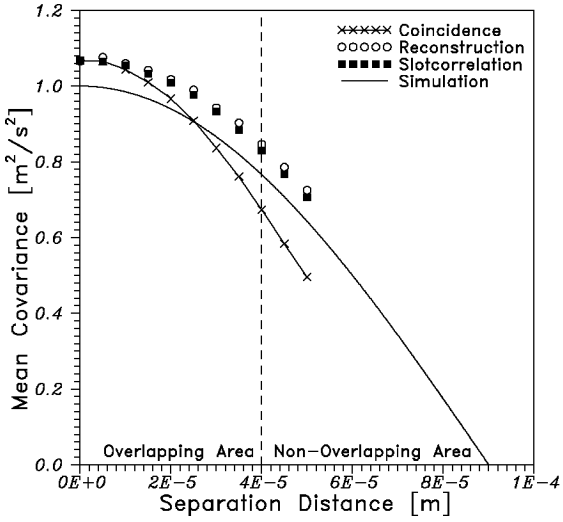

Figure 5: Mean covariance estimated for case 2: f-type correlation at high turbulence.

reconstruction estimate, however the data rate decreases dramatically, as seen in figure 6c. Consequently, the estimator variance is also very high (figure 6b).

The reconstruction estimate is very close to the prescribed correlation at small separations but lies below at high separation values. This is related to the spatial averaging over the finite size of the two measurement volumes, an effect which is not present in the f-type correlation. This effect can be evaluated as a spatial integral

$$c_{AB}^{(m)} = \int_{\Delta y-2c}^{\Delta y+2c} \sigma_u^2 \cos\frac{y}{L_y} p(y)\, dy \qquad (9)$$

where $\sigma_u^2 \cos\frac{y}{L_y}$ is the prescribed spatial correlation and where the probability of the y value of the particle passage is uniform across the volume

$$p(y) = \frac{1 - \left|\frac{y-\Delta y}{2c}\right|}{\int_{\Delta y-2c}^{\Delta y+2c} \left(1 - \left|\frac{y-\Delta y}{2c}\right|\right)\, dy} \qquad (10)$$

The value of $c_{AB}^{(m)}$ has been added to figure 6a and describes the reconstruction estimator well at larger lag times. At very small lag times single particle, two channel signals dominate and the true zero correlation is estimated.

The slot correlation exhibits both the spatial averaging mentioned above and the temporal averaging over the slot width and lies therefore below the reconstruction estimate.

As in previous cases, the reconstruction also exhibits the lowest variance, as seen in figure 6b.

Finally results for the g-type correlation at high turbulence levels is shown in figure 7. As in case 2, a systematic error of the covariance is apparent for the reconstruction and slot estimates. The lower variance of the reconstruction estimate is even more pronounced. The data rate behavior is similar to that in case 3. (figure 6c).

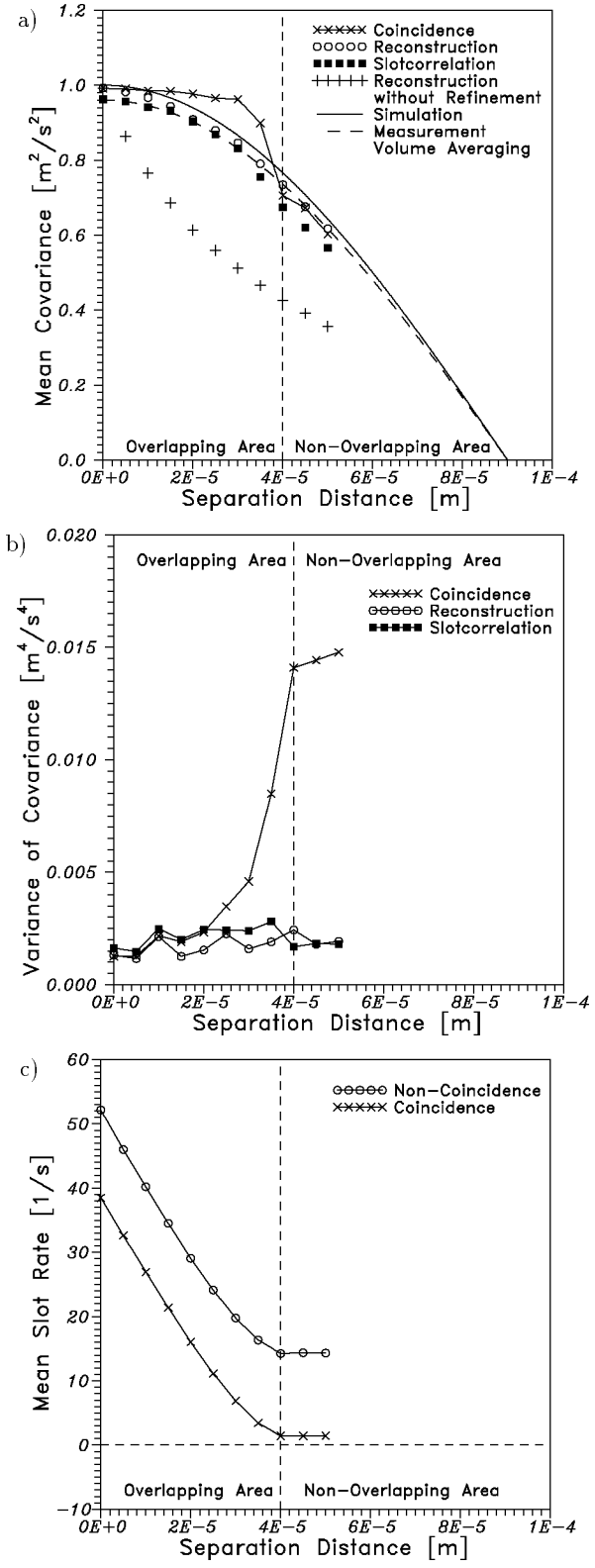

Figure 6: Results for case 3: low turbulence, g-type correlation.

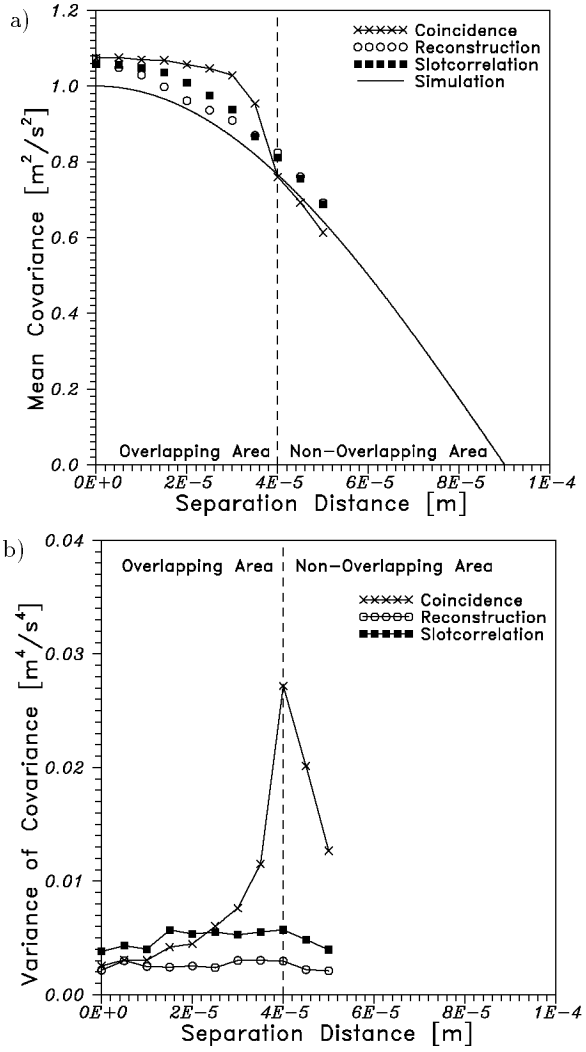

Figure 7: Results for case 4: high turbulence, g-type correlation.

Practically, the lower variance exhibited by the slot correlation and reconstruction estimate should allow shorter measurement times to achieve a given uncertainty. This has been more explicitly investigated by computing the estimators' variances as a function of particle concentration and also measurement time. The results are presented in figures 8a and b respectively, using the flow parameters of case 3.

Included in these figures are results using 3 coincidence window widths, between 1 ms and 10 ms. The 10 ms window corresponds to the slot width employed, however already leads to a reduced (biased) correlation. The 1 ms window is more realistic. For a given variance, the slot correlation or reconstruction estimate leads to measurement times of a factor 5 less than with the coincidence estimate. Similarly, the slot correlation and reconstruction estimate achieve a given variance at much lower particle concentrations, for a fixed measurement time. Indeed, at very low particle concentrations the slot correlation outperforms the reconstruction estimate. This lies presam-

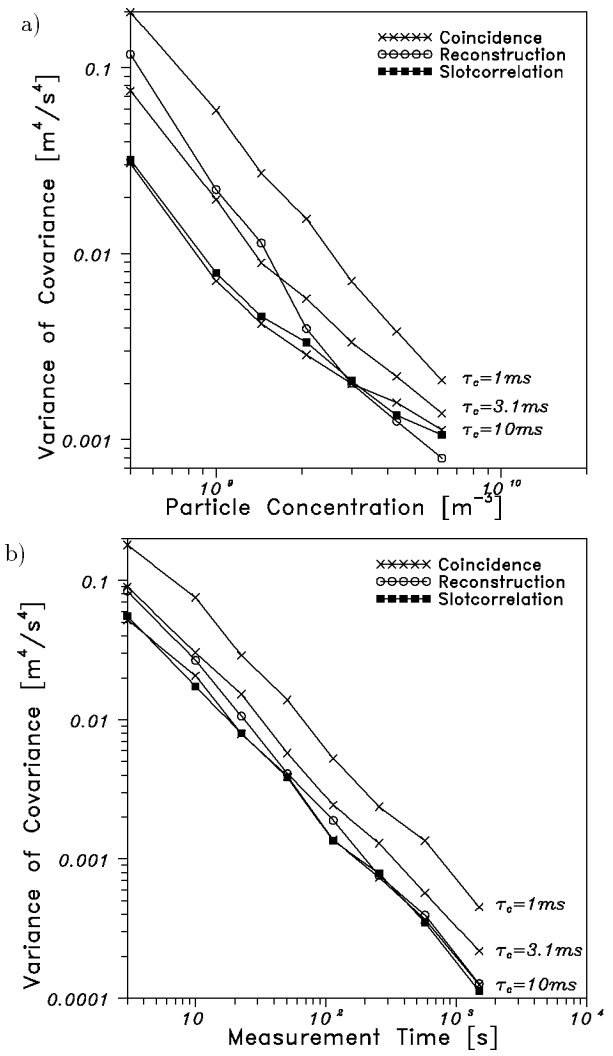

Figure 8: Estimators' variance for case 3: low turbulence, g-type correlation.

ably in the fact that at vary low particle concentrations, the particle rate $\dot{n}$, required for the refinement step, is poorly estimated. In either case however, the improvement factor is much less than for the measurement time.

Note that figure 8a and b are both plotted in a double logarithmic scale, indicating the power law behavior of the variance as a function of particle concentration and measurement time.

5. CONCLUSIONS

The present results indicate clearly the advantages of the slot correlation and the reconstruction estimate over a coincidence estimate for the cross- correlation of velocity data from a two-point LDA. For the user the main advantage lies in a significantly shorter measurement duration to achieve a given variance, typically a factor of 5 or larger. Furthermore the spatial bias for overlapping measurement volumes is completely avoided.

The reconstruction technique shows less systematic error than the slot correlation and furthermore has a lower variance. On the other hand the slot correlation is significantly easier to implement, requires less computational time and is also robust when the particle concentration varies significantly. The main disadvantage of the slot correlation is the inherent time averaging over each slot width.

6. ACKNOWLEDGEMENTS

Funding from the Deutsche Forschungsgemeinschaft under grants Tr 194/9 and Mu 1117/1 is gratefully acknowledged.

REFERENCES

[1] Adrian, R. J.; Yao, C. S.: *Power Spectra of Fluid Velocities Measured by Laser Doppler Velocimetry.* Exp. in Fluids **5** (1987), 17–28.

[2] Benedict, L. H.; Gould, R. D.: *Understanding biases in the near-field region of LDA two-point correlation measurements.* Proc. 8th Int. Symp. of Appl. of Laser Techn. to Fluid Mechanics, Lisbon, Portugal (1996), paper 36.6.

[3] Fuchs, W.; Albrecht, H.; Nobach, H.; Tropea, C.;Graham, L. J. W.: *Simulation and Experimental Verification of Statistical Bias in Laser Doppler Anemometry including Non-Homogeneous Particle Density.* Proc. 8th Int. Symp. on Appl. of Laser Techn. to Fluid Mechanics, Lisbon, Portugal (1992), paper 36.2.

[4] Müller, E.; Nobach, H.; Tropea, C.: *A Refined Reconstruction-based Correlation Estimator for Two- channel, Non-coincidence Laser Doppler Anemometer.* Measurement Science and Technology, vol. 9 (1998), no. 3, pp. 442–451.

[5] Nobach H.: *Verarbeitung stochastisch abgetasteter Signale — Anwendung in der Laser-Doppler-Anemometrie.* Shaker Verlag Aachen, 1998 (Berichte aus der Lasertechnik), also Rostock, Univ., Diss., 1997, ISBN 3-8265-3332-1.

[6] Nobach, H.; Müller, E.; Tropea, C.: *Efficient estimation of power spectral density from laser Doppler anemometer data.* Experiments in Fluids, vol. 24 (1998), no. 5/6, pp. 499–509.